Topological SQUIPT Based on Helical Edge States in Proximity to Superconductors

Lennart Bours,[1,*] Björn Sothmann,[2] Matteo Carrega,[1] Elia Strambini,[1] Ewelina M. Hankiewicz,[3] Laurens W. Molenkamp,[4] and Francesco Giazotto[1]

[1] *NEST, Istituto Nanoscienze–CNR and Scuola Normale Superiore, Piazza San Silvestro 12, 56127 Pisa, Italy*

[2] *Theoretische Physik, Universität Duisburg-Essen and CENIDE, D-47048 Duisburg, Germany*

[3] *Institute for Theoretical Physics and Astrophysics, University of Würzburg, Am Hubland, D-97074 Würzburg, Germany*

[4] *Experimentelle Physik 3, Physikalisches Institut, University of Würzburg, Am Hubland, D-97074 Würzburg, Germany*

(Received 31 January 2018; revised manuscript received 8 May 2018; published 25 July 2018)

We propose a device based on a topological Josephson junction where the helical edge states of a two-dimensional (2D) topological insulator are in close proximity to two superconducting leads. The presence of a magnetic flux through the junction leads to a Doppler shift in the spectrum of Andreev bound states, and affects the quantum interference between proximized edge states. We inspect the emergent features, accessing the density of states through a tunnel-coupled metallic probe, thus realizing a topological superconducting quantum-interference-proximity transistor (TSQUIPT). We calculate the expected performance of this device, concluding that it can be used as a sensitive absolute magnetometer due to the voltage drop across the junction decaying to a constant value as a function of the magnetic flux. Contrary to conventional SQUID and SQUIPT designs, no ring structure is needed. The findings pave the way for sensitive hybrid devices that exploit the helical edge states of a 2D topological insulator.

DOI: 10.1103/PhysRevApplied.10.014027

I. INTRODUCTION

The past decade has seen immense interest in the physics of topological insulators (TIs), motivated by their potential applications in nanoelectronics, spintronics, and quantum computation [1–5]. The existence of both two-dimensional (2D) and three-dimensional (3D) TIs was predicted roughly ten years ago [6–13] and was confirmed experimentally shortly afterwards via transport [14] and spectroscopic measurements [15,16]. Two-dimensional TIs have been realized in HgTe/CdTe [14,17–20] and InAs/GaSb [21–27] quantum wells that exhibit an insulating behavior in the bulk while transport properties are governed by topologically protected gapless edge states. Due to the strong spin-orbit coupling, the spin and momentum degrees of freedom in the edge states are locked, resulting in helical edge channels [28]. This means that each surface of a 2D TI hosts one pair of counter-propagating edge states with opposite spin [18]. The helical edge states are protected against backscattering by time-reversal symmetry, which guarantees robustness against several kinds of disorder and perturbations. A large number of studies have been put forward on the nature of helical edge states of TIs, including the role of *e*-*e* interactions [29–31], breaking of time-reversal symmetry [32–34], and spin properties [35].

Superconducting correlations can be induced in edge channels via the proximity effect from a conventional superconductor [36–42]. The induced superconductivity exhibits both spin-singlet s-wave pairing as well as spin-triplet p-wave pairing due to the strong spin-orbit coupling in the TI. In a topological Josephson junction where two superconducting electrodes are coupled to each other via the edge states of a TI, the presence of p-wave pairing opens up the possibility of creating Majorana modes in the form of topologically protected zero-energy Andreev bound states [43,44]. These Majorana modes could give rise to a 4π-periodic Josephson current [45–48], feature that has recently been observed experimentally [49–51]. Furthermore, they are responsible for an anomalous current-phase relation [52,53] and can be identified by their unique phase-dependent thermal conductance [54].

Additional control over the gapless Andreev bound states can be obtained by applying a small magnetic flux through a ballistic 2D topological Josephson junction. The magnetic flux induces a local gradient of the superconducting phase, resulting in a finite Cooper-pair (condensate) momentum along the edge, p_S. This modifies the amplitude for Andreev reflections in which an incident electron (hole)

*lennart.bours1@sns.it

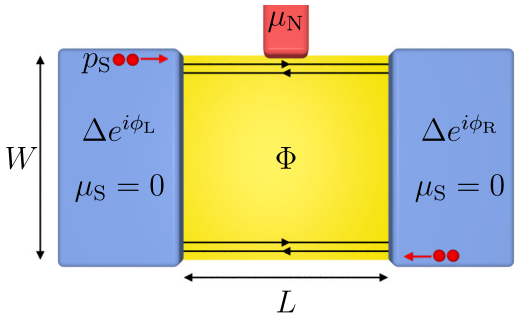

FIG. 1. A schematic illustration of the proposed device. A topological Josephson junction is formed by two superconducting leads (blue) coupled via a 2D topological insulator (yellow) of width W and length L. Transport through the topological insulator occurs via two helical edge states at the boundary of the insulator. A normal probe terminal (red) is tunnel coupled to the edge states via a tunnel barrier. A magnetic flux Φ through the junction gives rise to a finite Cooper-pair momentum p_S in the superconducting leads.

from the edge state is reflected as a hole (electron) and, thus, modifies the spectrum of the Andreev bound states forming inside the junction as well as the transport properties of the junction [55]. In fact, the electrons at the upper and lower edges acquire different momentum shifts under Andreev reflection due to the opposite signs of a finite Cooper-pair momentum shift, an effect similar to Doppler shift. This allows for closing of the induced superconducting gap by small magnetic fields of a few mT, which do not suppress the helical edge conductance [56].

This effect can be exploited, for instance, to manipulate the thermal conductance of the junction. While the thermal conductance is exponentially suppressed in the presence of a superconducting gap, it is twice the thermal-conductance quantum when the gap is closed and both edge channels contribute to energy transport. This enables the operation of such a device as a thermal switch [57,58].

In this work, we propose a device to investigate the quantum interference of edge supercurrents in 2D TIs. The quantum interference of supercurrents carried by the two edges of the Josephson junction has been studied by analyzing their flux dependence [55,59]. Here, we aim to probe the density of states of a single proximized edge via a normal tunnel probe (see Fig. 1). In essence, the proposed device realizes a topological variant of the superconducting quantum interference proximity transistor [60–74], or TSQUIPT. We characterize the TSQUIPT and its performance, and present calculations of the expected device behavior in transport experiments.

Not only does the TSQUIPT host physics that is interesting for fundamental reasons, but it can also be used as an absolute magnetometer due to its nonperiodic flux dependence; by tracing the device's response to an applied flux, one can determine the absolute flux, and by extension the magnetic field to which the device is exposed. Contrary to other flux-sensitive devices, no ring structure is needed, which is advantageous with regards to fabrication, and the device sensitivity can be tuned via a bias current.

The paper is organized as follows. In Sec. II, we summarize the model and sketch the basic equations for helical edge states in proximity to two superconductors. These are then used to derive the expression for the density of states, which will be investigated in detail in Sec. III by inspecting the transport properties of a tunnel-coupled metallic probe. The electrical response of the TSQUIPT will be presented, together with the implementation of an absolute magnetometer, with an optimum sensitivity comparable to state-of-the-art commercial SQUIDs. Future prospects are discussed and results are summarized in Sec. IV.

II. MODEL AND BASIC DEFINITIONS

We consider a topological Josephson junction consisting of two superconducting electrodes connected by a 2D TI of length L and width W, as depicted in Fig. 1. We assume that the width of the 2D TI is so large that an overlap or coherent coupling [59] between edge channels from different edges can safely be neglected. Increasing the width of the device does not negatively influence the behavior or performance of the proposed device. A normal metal probe is weakly tunnel coupled to the upper edge of the junction. Assuming that both superconductors are kept at the same electrochemical potential $\mu_S = 0$, one can inject a charge current from the probe into the Josephson junction by applying a bias voltage $V = \mu_N/e$ to the probe terminal.

The left (L) and right (R) superconducting leads are characterized by a superconducting order parameter $\Delta e^{i\phi_{L,R}}$. We assume that the order parameter changes at the superconductor–topological insulator interface on a length scale shorter than the superconducting coherence length $\xi_0 = \hbar v_F/\Delta$, with the Fermi velocity v_F, which allows us to model the spatial variation of the order parameter as $\Delta(x) = \Delta[\Theta(-x - L/2)e^{i\phi_L} + \Theta(x - L/2)e^{-i\phi_R}]$, where $\Theta(x)$ is the step function. We neglect proximity effects inside the junction that would require a self-consistent evaluation of the order parameter. This is a reasonable approximation since transport through the junction proceeds via the two edge channels only [75]. The proximized noninteracting helical edge states [76] at the upper edge are described by the Bogoliubov–de Gennes Hamiltonian

$$H_{\mathrm{BdG}} = \begin{pmatrix} h(x) & i\sigma_y\Delta(x) \\ -i\sigma_y\Delta(x)^* & -h^*(x) \end{pmatrix}. \tag{1}$$

In the above equation, $\Delta(x)$ is the superconducting pairing potential, while the diagonal terms describe the two edge channels and read

$$h(x) = v_F\sigma_x\left(-i\hbar\partial_x + \frac{p_S}{2}\right) + \sigma_0\mu, \tag{2}$$

where v_F is the Fermi velocity, σ_0 is the identity matrix, the σ_j are the Pauli matrices acting on spin space, and μ is the chemical potential. We have introduced

$$p_S = \frac{\pi \xi_0 \Delta}{v_F L} \frac{\Phi}{\Phi_0}, \tag{3}$$

which denotes a finite Cooper-pair (condensate) momentum along the edge. When the normal lead is attached, as in Fig. 1, it can inject right-propagating electrons with momentum p and left-propagating electrons with momentum $-p$, both acquiring the same momentum shift $p_S/2$ during Andreev reflection (for the upper edge), leading to a relative momentum shift for left and right movers similar to the well-known Doppler shift. $\Phi = WLB$ is the flux through the junction and Φ_0 is the magnetic flux quantum.

The Cooper-pair momentum relevant for transport properties along the edge channels is determined by the width of the 2D TI weak link as long as the superconductor width exceeds that of the TI. As we take W much larger than the spatial extension of the edge states, the Cooper-pair momentum is taken to be the boundary value. The magnetic field is assumed to be sufficiently small such that no backscattering is induced in the helical edge channels [77], and superconductivity is not quenched in the leads. In addition to inducing a finite Cooper-pair momentum, the magnetic field also leads to a coordinate dependence of the phase difference $\phi_R - \phi_L$. Taking the junction to be smaller than the Josephson penetration depth (which is a good approximation for nanoscale junctions), we obtain for the phase difference across the upper edge $\phi_u = \phi_0 + \pi(\Phi/\Phi_0)$, where ϕ_0 denotes the phase difference in the absence of a magnetic flux.

The eigenfunctions of the Bogoliubov–de Gennes Hamiltonian in an infinite superconductor with phase ϕ_i are given, in Nambu notation, by

$$\psi_1(x) = (u_-, u_-, -e^{-i\phi_i} v_-, e^{-i\phi_i} v_-)^T e^{ik_e x}, \tag{4}$$

$$\psi_2(x) = (v_-, v_-, -e^{-i\phi_i} u_-, e^{-i\phi_i} u_-)^T e^{ik_h x}, \tag{5}$$

$$\psi_3(x) = (u_+, -u_+, e^{-i\phi_i} v_+, e^{-i\phi_i} v_+)^T e^{-ik_e x}, \tag{6}$$

$$\psi_4(x) = (v_+, -v_+, e^{-i\phi_i} u_+, e^{-i\phi_i} u_+)^T e^{-ik_h x}, \tag{7}$$

describing right-moving electronlike, left-moving holelike, left-moving electronlike, and right-moving holelike quasiparticles, respectively. In the above equations, we have introduced

$$u_\pm = \frac{1}{2}\left(1 + \frac{\sqrt{E_\pm^2 - |\Delta|^2}}{E_\pm}\right), \tag{8}$$

$$v_\pm = \frac{1}{2}\left(1 - \frac{\sqrt{E_\pm^2 - |\Delta|^2}}{E_\pm}\right), \tag{9}$$

where $E_\pm = E \pm v_F p_S/2$ and $k_{e,h}$ is the wave vector associated with the electron- and holelike quasiparticles, respectively. To find the wave function in all three regions, we consider the wave-matching approach at the Superconductor-2D TI interfaces assuming, for simplicity, ideally transparent interfaces. Let us consider the case of an electronlike quasiparticle impinging on the junction from the left. The wave functions in the three different regions, i.e., the left superconductor (S, l), the central topological region (2D TI), and the right superconductor (S, r) of the junction, can be written as

$$\psi_{S,l}(x) = \psi_1(x) + r_e \psi_3(x) + r_h \psi_2(x), \tag{10}$$

$$\psi_{2D\,TI}(x) = \sum_i a_i \psi_i(x), \tag{11}$$

$$\psi_{S,r}(x) = t_e \psi_1(x) + t_h \psi_4(x). \tag{12}$$

Here, r_e, r_h, t_e, and t_h represent the reflection and transmission coefficients for electronlike and holelike quasiparticles. Taking into account the continuity of the wave function at the interfaces, we obtain the wave function in the central region, which provides direct access to the transmission probability of quasiparticles through the junction. We remark that while the normal-state transmission of a 2D TI equals unity due to Klein tunneling preventing backscattering in the presence of time-reversal symmetry, the transmission in the superconducting state depends on energy, phase difference, and magnetic flux in a nontrivial way, due to interference effects [57]. These quantum interferences also manifest themselves in the density of states of the junction. Writing the wave function of the central region as $\psi_{2D\,TI} = (u_\uparrow, u_\downarrow, v_\uparrow, v_\downarrow)$, the corresponding contribution to the density of states of the upper edge channel inside the junction is given by

$$\rho(E) = \sum_{k,\sigma,\eta=\pm} [|u_\sigma|^2 \delta(E - E_{k\eta}) + |v_\sigma|^2 \delta(E + E_{k\eta})], \tag{13}$$

where we define $E_{k\pm} = \sqrt{(v_F k \pm \mu)^2 + \Delta^2} \pm v_F p_S/2$. The $+$ and $-$ refer to left- and right-moving quasiparticles, respectively. Due to the counter-propagating nature of

helical edge states, the left and right movers are shifted opposite in energy by $\pm(v_F p_S/2)$.

Including the contributions for quasiparticles of both types impinging from the right-hand side and performing the sum over momenta, we obtain the density of states $\rho(E)$ of the 2D topological Josephson junction in units of $\rho_{\rm EC} = (\pi\hbar v_F)^{-1}$, the density of states per unit volume of a single edge channel. For energies above the superconducting gap, we find that

$$\rho(E) = \sum_{\sigma=\pm} \rho_{\rm BCS}(E_\sigma) F_\sigma(E_\sigma), \tag{14}$$

where

$$\rho_{\rm BCS}(E) = \frac{|E|}{\sqrt{|E|^2 - \Delta^2}} \Theta(|E| - \Delta) \tag{15}$$

is the Bardeen-Cooper-Schrieffer (BCS) density of states. The function

$$F_\pm(E) = \frac{E^2 - \Delta^2}{E^2 - \Delta^2 \cos^2\left(\frac{\phi_u}{2} \pm \frac{EL}{\Delta\xi_0}\right)} \tag{16}$$

is a modulating function that arises due to quantum interference. We underline that the energy-dependent term inside the cosine arises from the energy dependence of the electronlike and holelike wave vectors and, from a physical point of view, reflects an additional phase picked up by an electron-hole pair making a round trip through the junction. Note that the density of states inside the gap can be obtained from Eq. (14) in a standard way via the analytic continuation $E \to E + i0^+$, and can be expressed in an analogous form.

The proximity-induced density of states (cf., Fig. 2) shows interesting features that are worth discussing in detail. As one can argue from the above expression, the full density of states is given by a sum of two BCS-like contributions, shifted in energy in opposite directions, with a modulating factor closely linked to quantum-interference effects.

Looking at Fig. 2, one can see that in the central diamond, energies are smaller than the superconducting gap and both channels are closed. Inside this region, sharp discrete peaks appear in the density of states due to the formation of Andreev bound states inside the junction. In the dark-blue diagonal arms, one of the two channels is opened due to an interplay between the particle energy and the Doppler shift that arises from the applied flux. The slope α of the arms is inversely proportional to the device length, $\alpha = \pm(1/L)(\pi\xi_0\Delta/v_F\Phi_0)$.

For large magnetic fluxes, light-blue regions form. Here, both channels are opened as the Doppler shift becomes larger than the gap. In addition, for large energies, both channels are open since the electronlike (holelike) energy exceeds the induced superconducting gap. An additional modulation appears in the density of states (more noticeable for long junctions), which stems from the energy dependence of the electronlike and holelike wave vectors. The slope of these oscillations is twice that of the arms themselves.

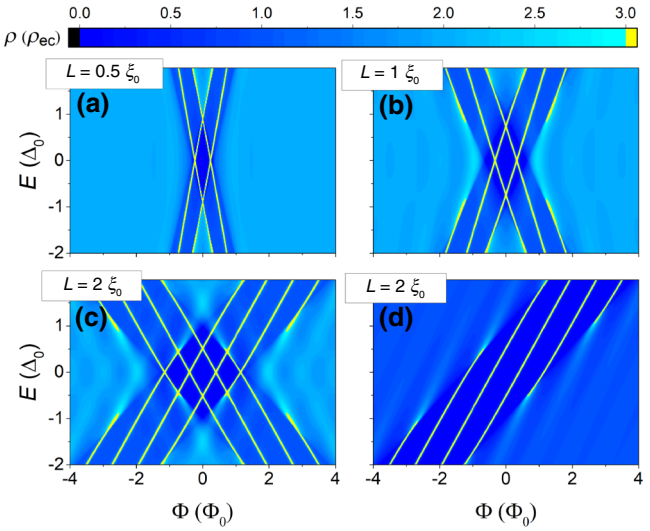

FIG. 2. The density of states of the topological Josephson junction as a function of energy, in units of the density of states of a single edge channel in its normal state, and the magnetic flux, in units of the flux quantum. Andreev bound states appear as sharp lines inside the gapped regions and transform into broad decaying resonances outside the gap. The superconducting phase difference without flux is $\phi_0 = 0$ for all plots. The complete density of states is shown for a junction length of (a) $L = 0.5\xi_0$, (b) $L = \xi_0$, and (c),(d) $L = 2\xi_0$. In (d), the contribution to the density of states of left movers alone is shown.

The density of states depends on the various system parameters in a nontrivial way. Increasing the junction

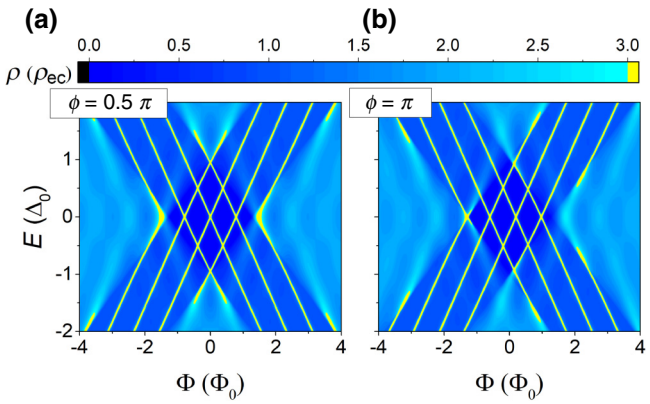

FIG. 3. The density of states of the topological Josephson junction for a junction length of $L = 2\xi_0$ with (a) the superconducting phase difference $\phi_0 = \pi/2$ and (b) $\phi_0 = \pi$. The ϕ_0 dependence is 2π-periodic and shifts the position of the Andreev bound states.

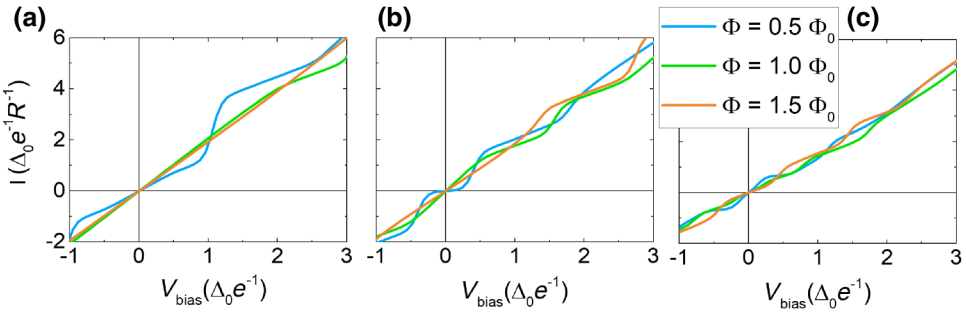

FIG. 4. The I-V characteristics at various fluxes. Different panels correspond to different junction lengths: (a) $L = 0.5\xi_0$; (b) $L = \xi_0$; (c) $L = 2\xi_0$. All curves are calculated for a temperature $T/T_C = 0.1$, where T_C denotes the critical temperature of the superconductors. The current and bias voltage are normalized in units of the superconducting gap at zero temperature, Δ_0, the electron charge e and the tunnel-junction resistance R.

length L while keeping its width W and the magnetic field B fixed leads to a linear increase of Φ. Furthermore, both the frequency and the strength of the oscillations arising from the energy dependence of wave vectors increase. Similarly, increasing the junction width W at constant L and B gives rise to an increased flux as well as to a growing Cooper-pair momentum p_S. Finally, changing B at fixed L and W yields a change of both the magnetic flux and the Cooper-pair momentum. Further control over the density of states can be obtained by tuning the phase difference ϕ_0. It can be exploited to move the BCS singularities in the density of states as shown in Fig. 3. Experimentally, ϕ_0 can be controlled by imposing a supercurrent between the superconducting leads or, alternatively, by closing the two leads in a loop. In the latter case, the magnetic field also determines ϕ_0 through flux quantization. In the following discussion, for the sake of clarity, we restrict the discussion to $\phi_0 = 0$, the extension to finite ϕ_0 being straightforward.

III. DEVICE CHARACTERISTICS

In order to probe the density of states in the topological edge channels, we consider a normal metal probe coupled to the side of the TI (see Fig. 1). We will focus on a weakly tunnel-coupled probe with a constant density of states equal to unity. In the following, we thus characterize the proposed TSQUIPT and its performance in view of future implementation by analyzing the charge current injected from the probe terminal for different lengths, temperatures, and fluxes and different biasing conditions. The general expression for the charge current injected from the

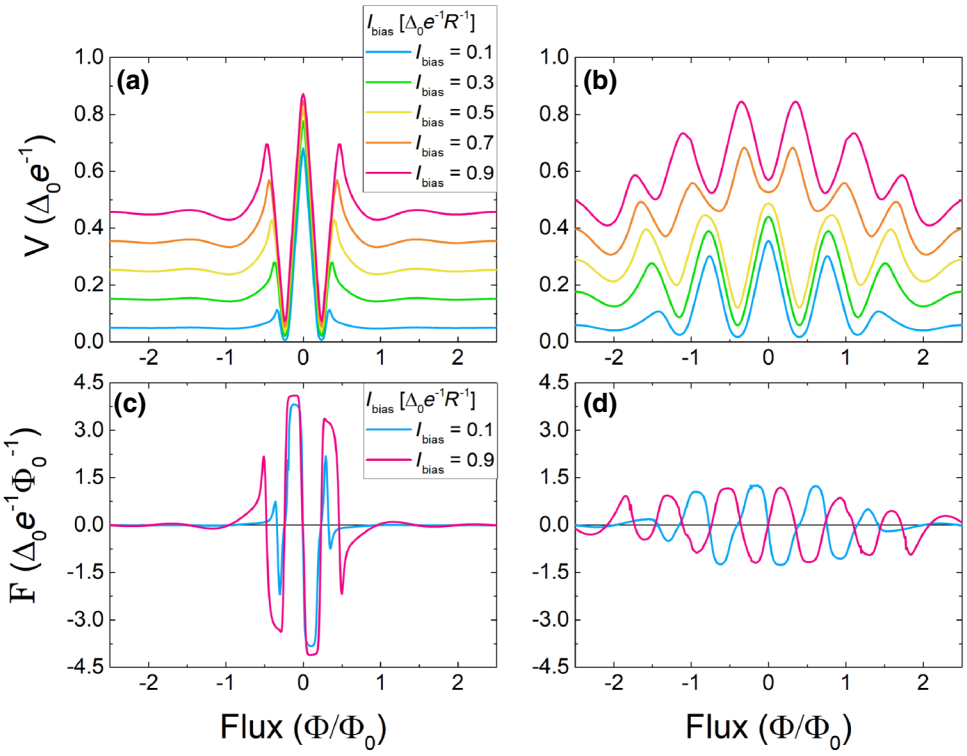

FIG. 5. (a),(b) The voltage drop across the device as a function of the flux for several values of the bias current, for junctions of length $L = 0.5\xi_0$ and $L = 2\xi_0$, respectively. (c),(d) The corresponding transfer function $dV/d\Phi$ for high- and low-bias currents, for junctions of length $L = 0.5\xi_0$ and $L = 2\xi_0$, respectively. All curves are calculated for a temperature $T/T_C = 0.1$.

tunnel probe is given by [78]

$$I(V) = \frac{1}{eR}\int dE\rho(E)\left[f_N(E) - f_S(E)\right], \qquad (17)$$

where $f_i(E) = \{\exp[(E-\mu_i)/(k_BT)]+1\}^{-1}$ denotes the Fermi functions of the normal probe ($i = N$) and the superconductors ($i = S$), respectively, and R is the resistance of the tunnel barrier. The resulting charge current is plotted in Fig. 4 for various junction lengths and fluxes. Due to the Andreev bound states, the conduction is almost never zero. It is shown that a smaller flux is required to open both channels in the case of short junctions. This is a result of comparing junctions of different length, but of the same width. Thus, the same flux through a shorter junction translates to a higher magnetic field and a higher Cooper-pair momentum p_s. In the regions where only one channel contributes to transport, the slope dI/dV is halved.

In the following, for the sake for clarity, we restrict ourselves to the case in which the device is operated via a current bias. Figure 5 shows the potential difference between the probe and the superconductors as a function of flux for several bias currents, as well as the voltage-to-flux transfer function

$$\mathcal{F} = \frac{\partial V}{\partial \Phi} \qquad (18)$$

for junctions of different length. The calculated transfer function compares favorably to a state-of-the-art SQUIPT [63], which can reach up to 0.4 mV/Φ_0 or $2(\Delta_0/e\Phi_0)$, with $\Delta_0 \approx 200$ μeV, the gap for aluminum, taken as a reference. The transfer functions change sign multiple times, and are damped at higher fluxes.

As shown in Fig. 5, the voltage drop across the device depends strongly on the magnetic flux for low flux, and tends to a finite value at high flux. As the flux dependence of the TSQUIPT is not periodic, the proposed 2D topological Josephson junction device can be utilized as a type of *absolute* magnetometer. That is, by tracing the $V(\Phi)$ function, one can determine the absolute flux, and by extension the magnetic field to which the device is exposed. This is in stark contrast to conventional SQUID-based magnetometers, which have a 2π-periodic flux dependence. To quantify the device's flux sensitivity, we calculate the flux noise given by

$$\phi_{ns} = \frac{\sqrt{S_v}}{|\mathcal{F}(\Phi)|}, \qquad (19)$$

where $S_v = (\partial V/\partial I)S_I$, $S_I = 2eI\coth(eV/2k_BT)$ is the tunneling current noise, and $\mathcal{F}(\Phi)$ is the voltage-to-flux transfer function. The flux noise is shown in Fig. 6 for two junctions of different lengths and for several values of the flux, as a function of the applied bias current. Figure 7 shows the temperature dependence of the flux noise. The minimum value of the flux noise is of the order of 10^{-6} $\Phi_0/\mathrm{Hz}^{1/2}$. The curves exhibit large peaks, which

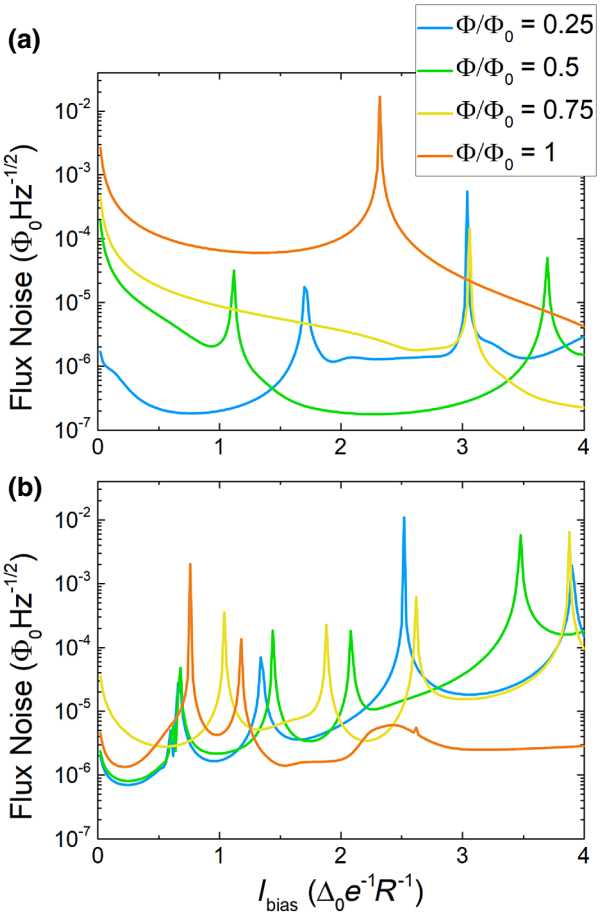

FIG. 6. The flux noise for various fluxes at a temperature of $T/T_C = 0.1$ and as a function of the bias current, for junctions of length (a) $L = 0.5\xi_0$ and (b) $L = 2\xi_0$.

are a consequence of the transfer function $\mathcal{F}(\Phi)$ regularly crossing zero. Note that the flux noise $\phi_{ns} \propto \sqrt{R}$, the tunnel-junction resistance, which we have taken to be 10 kΩ.

One advantage of the considered device is that, contrary to conventional SQUID and SQUIPT designs, no ring structure is needed for its implementation. The noise depends strongly on the zeroes in the transfer function, which can be controlled through ϕ_0 via an imposed supercurrent, allowing for easily optimized performance of the proposed device. The possibility of controlling the superconducting phase difference via a current bias is another advantage over conventional SQUID designs. While the behavior of the flux noise depends on the junction length, its width, the applied flux, and the temperature in a complicated way, the general rule is that a shorter junction performs better. The performance is ultimately limited by the technical ability to fabricate the junctions, and using state-of-the-art techniques the device has the potential to be extremely small, as the fundamental size limit is determined by the topological edge-channel width.

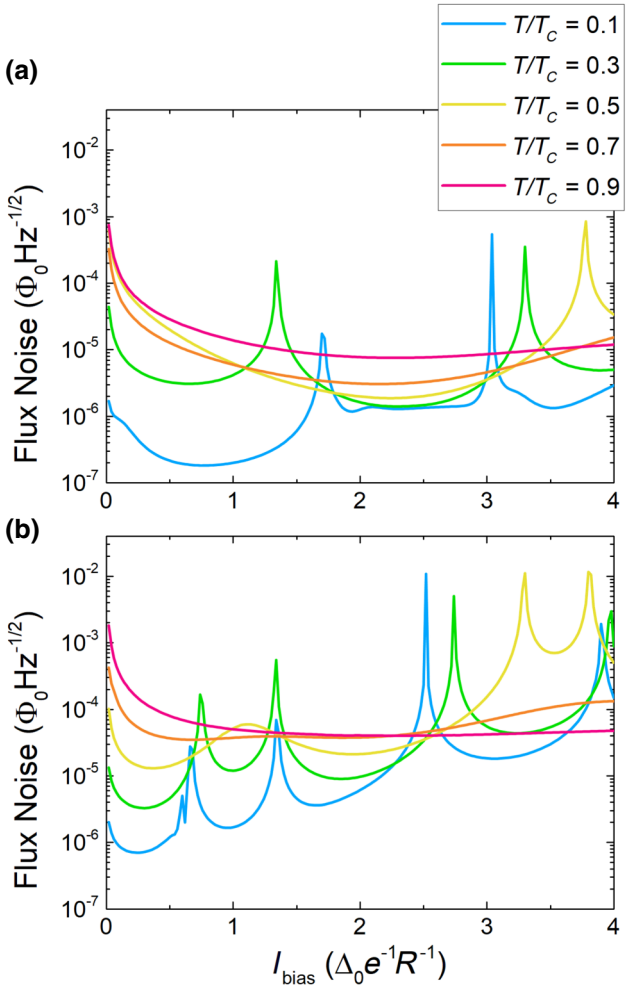

FIG. 7. The temperature dependence of the flux noise for a flux of $\Phi/\Phi_0 = 0.25$ as a function of the bias current, for junctions of length (a) $L = 0.5\xi_0$ and (b) $L = 2\xi_0$.

IV. SUMMARY AND CONCLUSIONS

We propose a topological SQUIPT, based on a 2D TI in close proximity to two superconductors, designed to investigate the subtle interplay between superconducting currents that arise in the presence of a small magnetic field and the helical edge states of a 2D TI. A weakly tunnel-coupled normal probe allows us to inspect the edge-channel density of states, which has a nontrivial energy and flux dependence. We conclude that the proposed device can be operated as a type of sensitive absolute magnetometer, which features several advantages over conventional SQUID and SQUIPT designs.

Understanding and verifying the electrical characteristics of this device will reinforce our knowledge of structures based on S-TI interfaces, and pave the way for more complex experiments that aim to exploit the quantum-interference phenomena present in these hybrid structures.

The proposed device is also interesting from a spintronics perspective; when only one channel is open, the current is spin polarized, due to the spin-momentum locking. This effect could be observed by replacing the normal metal probe with a spin-selective probe, e.g., a ferromagnetic tunnel-coupled probe.

ACKNOWLEDGMENTS

We acknowledge financial support from the Ministry of Innovation NRW. E. Strambini and F. Giazotto acknowledge financial support from ERC Grant Agreement No. 615187—COMANCHE. The work of F.G. was partially funded by the Tuscany Region under the FARFAS 2014 project SCIADRO. M.C. acknowledges support from the CNR-CONICET cooperation programme "Energy conversion in quantum, nanoscale, hybrid devices." E.M.H. and L.W.M. acknowledge financial support from the German Science Foundation (Leibniz Program, SFB1170 "ToCoTronics") and the Elitenetzwerk Bayern program "Topologische Isolatoren."

[1] M. Z. Hasan and C. L. Kane, Colloquium: Topological insulators, Rev. Mod. Phys. **82**, 3045 (2010).
[2] X.-L. Qi and S.-C. Zhang, Topological insulators and superconductors, Rev. Mod. Phys. **83**, 1057 (2011).
[3] M. Z. Hasan and J. E. Moore, Three-dimensional topological insulators, Annu. Rev. Cond. Mat. Phys. **2**, 55 (2011).
[4] Y. Ando, Topological insulator materials, J. Phys. Soc. Jpn. **82**, 102001 (2013).
[5] G. Tkachov and E. M. Hankiewicz, Spin-helical transport in normal and superconducting topological insulators, Phys. Status Solidi (b) **250**, 215 (2013).
[6] C. L. Kane and E. J. Mele, Quantum Spin Hall Effect in Graphene, Phys. Rev. Lett. **95**, 226801 (2005).
[7] C. L. Kane and E. J. Mele, Z_2 Topological Order and the Quantum Spin Hall Effect, Phys. Rev. Lett. **95**, 146802 (2005).
[8] B. A. Bernevig and S.-C. Zhang, Quantum Spin Hall Effect, Phys. Rev. Lett. **96**, 106802 (2006).
[9] B. A. Bernevig, T. L. Hughes, and S.-C. Zhang, Quantum spin Hall effect and topological phase transition in HgTe quantum wells, Science **314**, 1757 (2006).
[10] J. E. Moore and L. Balents, Topological invariants of time-reversal-invariant band structures, Phys. Rev. B **75**, 121306 (2007).
[11] L. Fu, C. L. Kane, and E. J. Mele, Topological Insulators in Three Dimensions, Phys. Rev. Lett. **98**, 106803 (2007).
[12] C. Liu, T. L. Hughes, X.-L. Qi, K. Wang, and S.-C. Zhang, Quantum Spin Hall Effect in Inverted Type-II Semiconductors, Phys. Rev. Lett. **100**, 236601 (2008).
[13] R. Roy, Topological phases and the quantum spin Hall effect in three dimensions, Phys. Rev. B **79**, 195322 (2009).
[14] M. König, S. Wiedmann, C. Brüne, A. Roth, H. Buhmann, L. W. Molenkamp, X.-L. Qi, and S.-C. Zhang, Quantum spin Hall insulator state in HgTe quantum wells, Science **318**, 766 (2007).

[15] D. Hsieh, D. Qian, L. Wray, Y. Xia, Y. S. Hor, R. J. Cava, and M. Z. Hasan, A topological Dirac insulator in a quantum spin Hall phase, Nature **452**, 970 (2008).
[16] Y. Xia, D. Qian, D. Hsieh, L. Wray, A. Pal, H. Lin, A. Bansil, D. Grauer, Y. S. Hor, R. J. Cava, and M. Z. Hasan, Observation of a large-gap topological-insulator class with a single Dirac cone on the surface, Nat. Phys. **5**, 398 (2009).
[17] A. Roth, C. Brüne, H. Buhmann, L. W. Molenkamp, J. Maciejko, X.-L. Qi, and S.-C. Zhang, Nonlocal transport in the quantum spin Hall state, Science **325**, 294 (2009).
[18] C. Brüne, A. Roth, H. Buhmann, E. M. Hankiewicz, L. W. Molenkamp, J. Maciejko, X.-L. Qi, and S.-C. Zhang, Spin polarization of the quantum spin Hall edge states, Nat. Phys. **8**, 485 (2012).
[19] K. C. Nowack, E. M. Spanton, M. Baenninger, M. König, J. R. Kirtley, B. Kalisky, C. Ames, P. Leubner, C. Brüne, H. Buhmann, L. W. Molenkamp, D. Goldhaber-Gordon, and K. A. Moler, Imaging currents in HgTe quantum wells in the quantum spin Hall regime, Nat. Mater. **12**, 787 (2013).
[20] M. König, M. Baenninger, A. G. F. Garcia, N. Harjee, B. L. Pruitt, C. Ames, P. Leubner, C. Brüne, H. Buhmann, L. W. Molenkamp, and D. Goldhaber-Gordon, Spatially Resolved Study of Backscattering in the Quantum Spin Hall State, Phys. Rev. X **3**, 021003 (2013).
[21] I. Knez, R.-R. Du, and G. Sullivan, Evidence for Helical Edge Modes in Inverted InAs/GaSb Quantum Wells, Phys. Rev. Lett. **107**, 136603 (2011).
[22] F. Nichele, A. N. Pal, P. Pietsch, T. Ihn, K. Ensslin, C. Charpentier, and W. Wegscheider, Insulating State and Giant Nonlocal Response in an InAs/GaSb Quantum Well in the Quantum Hall Regime, Phys. Rev. Lett. **112**, 036802 (2014).
[23] I. Knez, C. T. Rettner, S.-H. Yang, S. S. P. Parkin, L. Du, R.-R. Du, and G. Sullivan, Observation of Edge Transport in the Disordered Regime of Topologically Insulating InAs/GaSb Quantum Wells, Phys. Rev. Lett. **112**, 026602 (2014).
[24] F. Qu, A. J. A. Beukman, S. Nadj-Perge, M. Wimmer, B.-M. Nguyen, W. Yi, J. Thorp, M. Sokolich, A. A. Kiselev, M. J. Manfra, C. M. Marcus, and L. P. Kouwenhoven, Electric and Magnetic Tuning Between the Trivial and Topological Phases in InAs/GaSb Double Quantum Wells, Phys. Rev. Lett. **115**, 036803 (2015).
[25] T. Li, P. Wang, H. Fu, L. Du, K. A. Schreiber, X. Mu, X. Liu, G. Sullivan, G. A. Csáthy, X. Lin, and R.-R. Du, Observation of a Helical Luttinger Liquid in InAs/GaSb Quantum Spin Hall Edges, Phys. Rev. Lett. **115**, 136804 (2015).
[26] L. Du, I. Knez, G. Sullivan, and R.-R. Du, Robust Helical Edge Transport in Gated InAs/GaSb Bilayers, Phys. Rev. Lett. **114**, 096802 (2015).
[27] S. Mueller, A. N. Pal, M. Karalic, T. Tschirky, C. Charpentier, W. Wegscheider, K. Ensslin, and T. Ihn, Nonlocal transport via edge states in InAs/GaSb coupled quantum wells, Phys. Rev. B **92**, 081303 (2015).
[28] C. Wu, B. A. Bernevig, and S.-C. Zhang, Helical Liquid and the Edge of Quantum Spin Hall Systems, Phys. Rev. Lett. **96**, 106401 (2006).
[29] T. L. Schmidt, Current Correlations in Quantum Spin Hall Insulators, Phys. Rev. Lett. **107**, 096602 (2011).
[30] F. Ronetti, L. Vannucci, G. Dolcetto, M. Carrega, and M. Sassetti, Spin-thermoelectric transport induced by interactions and spin-flip processes in two-dimensional topological insulators, Phys. Rev. B **93**, 165414 (2016).
[31] A. Calzona, M. Acciai, M. Carrega, F. Cavaliere, and M. Sassetti, Time-resolved energy dynamics after single electron injection into an interacting helical liquid, Phys. Rev. B **94**, 035404 (2016).
[32] P. Delplace, J. Li, and M. Büttiker, Magnetic-Field-Induced Localization in 2D Topological Insulators, Phys. Rev. Lett. **109**, 246803 (2012).
[33] J. M. Edge, J. Li, P. Delplace, and M. Büttiker, Z_2 Peak of Noise Correlations in a Quantum Spin Hall Insulator, Phys. Rev. Lett. **110**, 246601 (2013).
[34] J. I. Väyrynen, M. Goldstein, and L. I. Glazman, Helical Edge Resistance Introduced by Charge Puddles, Phys. Rev. Lett. **110**, 216402 (2013).
[35] S. Das and S. Rao, Spin-Polarized Scanning-Tunneling Probe for Helical Luttinger Liquids, Phys. Rev. Lett. **106**, 236403 (2011).
[36] L. Maier, J. B. Oostinga, D. Knott, C. Brüne, P. Virtanen, G. Tkachov, E. M. Hankiewicz, C. Gould, H. Buhmann, and L. W. Molenkamp, Induced Superconductivity in the Three-Dimensional Topological Insulator HgTe, Phys. Rev. Lett. **109**, 186806 (2012).
[37] J. R. Williams, A. J. Bestwick, P. Gallagher, S. S. Hong, Y. Cui, A. S. Bleich, J. G. Analytis, I. R. Fisher, and D. Goldhaber-Gordon, Unconventional Josephson Effect in Hybrid Superconductor-Topological Insulator Devices, Phys. Rev. Lett. **109**, 056803 (2012).
[38] I. Knez, R.-R. Du, and G. Sullivan, Andreev Reflection of Helical Edge Modes in InAs/GaSb Quantum Spin Hall Insulator, Phys. Rev. Lett. **109**, 186603 (2012).
[39] J. B. Oostinga, L. Maier, P. Schüffelgen, D. Knott, C. Ames, C. Brüne, G. Tkachov, H. Buhmann, and L. W. Molenkamp, Josephson Supercurrent Through the Topological Surface States of Strained Bulk HgTe, Phys. Rev. X **3**, 021007 (2013).
[40] A. D. K. Finck, C. Kurter, Y. S. Hor, and D. J. Van Harlingen, Phase Coherence and Andreev Reflection in Topological Insulator Devices, Phys. Rev. X **4**, 041022 (2014).
[41] S. Hart, H. Ren, T. Wagner, P. Leubner, M. Mühlbauer, C. Brüne, H. Buhmann, L. W. Molenkamp, and A. Yacoby, Induced superconductivity in the quantum spin Hall edge, Nat. Phys. **10**, 638 (2014).
[42] V. S. Pribiag, A. J. A. Beukman, F. Qu, M. C. Cassidy, C. Charpentier, W. Wegscheider, and L. P. Kouwenhoven, Edge-mode superconductivity in a two-dimensional topological insulator, Nat. Nanotechnol. **10**, 593 (2015).
[43] L. Fu and C. L. Kane, Superconducting Proximity Effect and Majorana Fermions at the Surface of a Topological Insulator, Phys. Rev. Lett. **100**, 096407 (2008).
[44] G. Tkachov and E. M. Hankiewicz, Helical Andreev bound states and superconducting Klein tunneling in topological insulator Josephson junctions, Phys. Rev. B **88**, 075401 (2013).
[45] L. Fu and C. L. Kane, Josephson current and noise at a superconductor/quantum-spin-Hall-insulator/superconductor junction, Phys. Rev. B **79**, 161408 (2009).
[46] D. M. Badiane, M. Houzet, and J. S. Meyer, Nonequilibrium Josephson Effect Through Helical Edge States, Phys. Rev. Lett. **107**, 177002 (2011).

[47] C. W. J. Beenakker, D. I. Pikulin, T. Hyart, H. Schomerus, and J. P. Dahlhaus, Fermion-Parity Anomaly of the Critical Supercurrent in the Quantum Spin-Hall Effect, Phys. Rev. Lett. **110**, 017003 (2013).

[48] F. Crépin and B. Trauzettel, Parity Measurement in Topological Josephson Junctions, Phys. Rev. Lett. **112**, 077002 (2014).

[49] J. Wiedenmann, E. Bocquillon, R. S. Deacon, S. Hartinger, O. Herrmann, T. M. Klapwijk, L. Maier, C. Ames, C. Brüne, C. Gould, A. Oiwa, K. Ishibashi, S. Tarucha, H. Buhmann, and L. W. Molenkamp, 4π-periodic Josephson supercurrent in HgTe-based topological Josephson junctions, Nat. Commun. **7**, 10303 (2016).

[50] E. Bocquillon, R. S. Deacon, J. Wiedenmann, P. Leubner, T. M. Klapwijk, C. Brüne, K. Ishibashi, H. Buhmann, and L. W. Molenkamp, Gapless Andreev bound states in the quantum spin Hall insulator HgTe, Nat. Nanotechnol. **12**, 137 (2017).

[51] R. S. Deacon, J. Wiedenmann, E. Bocquillon, F. Domínguez, T. M. Klapwijk, P. Leubner, C. Brüne, E. M. Hankiewicz, S. Tarucha, K. Ishibashi, H. Buhmann, and L. W. Molenkamp, Josephson Radiation from Gapless Andreev Bound States in HgTe-Based Topological Junctions, Phys. Rev. X **7**, 021011 (2017).

[52] I. Sochnikov, L. Maier, C. A. Watson, J. R. Kirtley, C. Gould, G. Tkachov, E. M. Hankiewicz, C. Brüne, H. Buhmann, L. W. Molenkamp, and K. A. Moler, Nonsinusoidal Current-Phase Relationship in Josephson Junctions from the 3D Topological Insulator HgTe, Phys. Rev. Lett. **114**, 066801 (2015).

[53] C. Kurter, A. D. K. Finck, Y. S. Hor, and D. J. Van Harlingen, Evidence for an anomalous current-phase relation in topological insulator Josephson junctions, Nat. Commun. **6**, 7130 (2015).

[54] B. Sothmann and E. M. Hankiewicz, Fingerprint of topological Andreev bound states in phase-dependent heat transport, Phys. Rev. B **94**, 081407(R) (2016).

[55] G. Tkachov, P. Burset, B. Trauzettel, and E. M. Hankiewicz, Quantum interference of edge supercurrents in a two-dimensional topological insulator, Phys. Rev. B **92**, 045408 (2015).

[56] D. I. Pikulin, T. Hyart, S. Mi, J. Tworzydlo, M. Wimmer, and C. W. J. Beenakker, Disorder and magnetic-field-induced breakdown of helical edge conduction in an inverted electron-hole bilayer, Phys. Rev. B. **89**, 161403 (2014).

[57] B. Sothmann, F. Giazotto, and E. M. Hankiewicz, High-efficiency thermal switch based on topological Josephson junctions, New J. Phys. **19**, 023056 (2017).

[58] M. J. M. J. Martínez-Pérez, P. Solinas, and F. Giazotto, Coherent caloritronics in Josephson-based nanocircuits, J. Low. Temp. Phys. **175**, 813 (2014).

[59] B. Baxevanis, V. P. Ostroukh, and C. W. J. Beenakker, Even-odd flux quanta effect in the Fraunhofer oscillations of an edge-channel Josephson junction, Phys. Rev. B **91**, 041409 (2015).

[60] F. Giazotto, J. T. Peltonen, M. Meschke, and J. P. Pekola, Superconducting quantum interference proximity transistor, Nat. Phys. **6**, 254 (2010).

[61] M. Meschke, J. T. Peltonen, J. P. Pekola, and F. Giazotto, Tunnel spectroscopy of a proximity Josephson junction, Phys. Rev. B **84**, 214514 (2011).

[62] A. Ronzani, C. Altimiras, and F. Giazotto, Highly Sensitive Superconducting Quantum-Interference Proximity Transistor, Phys. Rev. Appl. **2**, 024005 (2014).

[63] S. D'Ambrosio, M. Meissner, C. Blanc, A. Ronzani, and F. Giazotto, Normal metal tunnel junction-based superconducting quantum interference proximity transistor, Appl. Phys. Lett. **107**, 113110 (2015).

[64] P. Virtanen, A. Ronzani, and F. Giazotto, Spectral Characteristics of a Fully Superconducting SQUIPT, Phys. Rev. Appl. **6**, 054002 (2016).

[65] E. Strambini, S. D'Ambrosio, F. Vischi, F. S. Bergeret, Yu. V. Nazarov, and F. Giazotto, The ω-SQUIPT as a tool to phase-engineer Josephson topological materials, Nat. Nano **11**, 1055 (2016).

[66] F. Vischi, M. Carrega, E. Strambini, S. D'Ambrosio, F. S. Bergeret, Yu. V. Nazarov, and F. Giazotto, Coherent transport properties of a three-terminal hybrid superconducting interferometer, Phys. Rev. B **95**, 054504 (2017).

[67] F. Giazotto and F. Taddei, Hybrid superconducting quantum magnetometer, Phys. Rev. B **84**, 214502 (2011).

[68] A. Ronzani, S. D'Ambrosio, P. Virtanen, F. Giazotto, and C. Altimiras, Phase-driven collapse of the Cooper condensate in a nanosized superconductor, Phys. Rev. B **96**, 214517 (2017).

[69] N. Ligato, G. Marchegiani, P. Virtanen, E. Strambini, and F. Giazotto, High operating temperature in V-based superconducting quantum interference proximity transistors, Sci. Rep. **7**, 8810 (2017).

[70] E. Enrico, E. Strambini, and F. Giazotto, Phase-driven charge manipulation in Hybrid Single-Electron Transistor, Sci. Rep. **7**, 13492 (2017).

[71] E. Enrico and F. Giazotto, Superconducting Quantum Interference Single-Electron Transistor, Phys. Rev. Appl. **5**, 064020 (2016).

[72] R. N. Jabdaraghi, D. S. Golubev, J. P. Pekola, and J. T. Peltonen, Noise of a superconducting magnetic flux sensor based on a proximity Josephson junction, Sci. Rep. **7**, 8011 (2017).

[73] R. N. J. Jabdaraghi, M. Meschke, and J. P. Pekola, Non-hysteretic superconducting quantum interference proximity transistor with enhanced responsivity, Appl. Phys. Lett. **104**, 082601 (2014).

[74] R. N. Jabdaraghi, J. T. Peltonen, O. -P. Saira, and J. P. Pekola, Low-temperature characterization of Nb-Cu-Nb weak links with Ar ion-cleaned interfaces, Appl. Phys. Lett. **108**, 042604 (2016).

[75] C. W. J. Beenakker, Universal Limit of Critical-Current Fluctuations in Mesoscopic Josephson Junctions, Phys. Rev. Lett. **67**, 3836 (1991).

[76] Here, for the sake of simplicity, we limit the discussion to the noninteracting case, neglecting possible e-e interactions within edge channels.

[77] G. Tkachov and E. M. Hankiewicz, Ballistic Quantum Spin Hall State and Enhanced Edge Backscattering in Strong Magnetic Fields, Phys. Rev. Lett. **104**, 166803 (2010).

[78] J. Bardeen, Tunnelling from a Many-Particle Point of View, Phys. Rev. Lett. **6**, 57 (1961).